

Old Dominion University

ODU Digital Commons

Electrical & Computer Engineering Faculty
Publications

Electrical & Computer Engineering

2021

Charge Transport, Conductivity and Seebeck Coefficient in Pristine and TCNQ Loaded Preferentially Grown Metal Organic Frameworks

Xin Chen
Old Dominion University


Kai Zhang

Zeinab Mohammed Hassan

Engelbert Redel

Helmut Baumgart
Old Dominion University, hbaumgar@odu.edu

Follow this and additional works at: https://digitalcommons.odu.edu/ece_fac_pubs

 Part of the [Electrical and Electronics Commons](#), and the [Polymer and Organic Materials Commons](#)

Original Publication Citation

Chen, X., Zhang, K., Hassan, Z. M., Redel, E., & Baumgart, H. (2021). Charge transport, conductivity and Seebeck coefficient in pristine and TCNQ loaded preferentially grown metal-organic framework films. *Journal of Physics: Condensed Matter Online* Article in Press, 1-20. <https://doi.org/10.1088/1361-648X/abe72f>

This Article is brought to you for free and open access by the Electrical & Computer Engineering at ODU Digital Commons. It has been accepted for inclusion in Electrical & Computer Engineering Faculty Publications by an authorized administrator of ODU Digital Commons. For more information, please contact digitalcommons@odu.edu.

ACCEPTED MANUSCRIPT • OPEN ACCESS

Charge Transport, Conductivity and Seebeck Coefficient in Pristine and TCNQ Loaded Preferentially Grown Metal-Organic Framework Films

To cite this article before publication: Xin Chen *et al* 2021 *J. Phys.: Condens. Matter* in press <https://doi.org/10.1088/1361-648X/abe72f>

Manuscript version: Accepted Manuscript

Accepted Manuscript is “the version of the article accepted for publication including all changes made as a result of the peer review process, and which may also include the addition to the article by IOP Publishing of a header, an article ID, a cover sheet and/or an ‘Accepted Manuscript’ watermark, but excluding any other editing, typesetting or other changes made by IOP Publishing and/or its licensors”

This Accepted Manuscript is © 2021 The Author(s). Published by IOP Publishing Ltd..

As the Version of Record of this article is going to be / has been published on a gold open access basis under a CC BY 3.0 licence, this Accepted Manuscript is available for reuse under a CC BY 3.0 licence immediately.

Everyone is permitted to use all or part of the original content in this article, provided that they adhere to all the terms of the licence <https://creativecommons.org/licenses/by/3.0>

Although reasonable endeavours have been taken to obtain all necessary permissions from third parties to include their copyrighted content within this article, their full citation and copyright line may not be present in this Accepted Manuscript version. Before using any content from this article, please refer to the Version of Record on IOPscience once published for full citation and copyright details, as permissions may be required. All third party content is fully copyright protected and is not published on a gold open access basis under a CC BY licence, unless that is specifically stated in the figure caption in the Version of Record.

View the [article online](#) for updates and enhancements.

Charge Transport, Conductivity and Seebeck Coefficient in Pristine and TCNQ Loaded Preferentially Grown Metal-Organic Framework Films

Xin Chen¹, Kai Zhang^{1,2}, Zeinab Mohamed Hassan³, Engelbert Redel^{*3} and Helmut Baumgart^{1,2*}

¹ Dept. Electrical and Computer Engineering, Old Dominion University, Norfolk, VA 23529, USA

² Applied Research Center, Newport News, Thomas Jefferson National Accelerator Lab, Virginia 23606, USA

³ Institute of Functional Interfaces (IFG), Karlsruhe Institute of Technology (KIT), Hermann-von-Helmholtz-Platz 1, 76344 Eggenstein-Leopoldshafen, Germany

This investigation on Metal-Organic Framework (MOF) HUKUST-1 films focuses on comparing the undoped pristine state and with the case of doping by TCNQ infiltration of the MOF pore structure. We have determined the temperature dependent charge transport p-type conductivity for HKUST-1 films. Furthermore, the electrical conductivity and the current-voltage characteristics have been characterized in detail. Because the most common forms of MOFs, bulk MOF powders, do not lend themselves easily to electrical characterization investigations, in this study the electrical measurements were performed on dense, compact surface-anchored metal-organic framework (SURMOF) films. These monolithic, well-defined, and (001) preferentially oriented MOF thin films are grown using quasi-liquid phase epitaxy (LPE) on specially functionalized silicon or borosilicate glass substrates. On pristine SURMOF films the effect of loading of these porous thin films with TCNQ has been investigated. Positive charge carrier conduction and a strong anisotropy in electrical conduction was observed for highly oriented SURMOF films and corroborated with Seebeck Coefficient measurements. Van der Pauw four-point Hall measurements provide important insight into the electrical behavior of such porous and hybrid organic-inorganic crystalline materials, which renders them attractive for potential use in microelectronic and optoelectronic devices and thermoelectric applications.

Organic Materials with tunable electrical properties are of considerable interest for the next generation of microelectronics, optoelectronic and thermoelectric devices. In the quest for new materials, hybrid compounds or organic heterolayers are being increasingly investigated regarding these potential applications.^[1] In this study, we focus on compact metal-organic framework (MOF) films, which are another class of hybrid material. MOFs are highly tunable and porous, and are also known as porous coordination polymers (PCPs).^[2] Metal-organic frameworks are formed by connecting organic linkers via inorganic metal (or metal/oxo) clusters.^[3,4] Due to their crystallinity, their thermal stability of typically up to 250°C and their open porous framework structure, this class of solids is highly adjustable and possesses interesting properties, which can be modulated and custom tailored.

1
2
3 For example, the sizes of the pores within MOFs have been reported to be highly tunable^[5], and
4 pore widths up to 10 nm have been reported,^[6] yielding porous solids with extremely low
5 densities. For the time being, bulk MOF powders constitute the de-facto standard modification
6 of MOF materials. The typical product of the most commonly applied solvothermal synthesis
7 method yields loosely packed bulk MOF powders, containing MOF crystallites with a
8 widespread size distribution up to the mm range. Determining the electrical properties and
9 characteristics of this class of solid porous materials with conventional methods for powders is
10 difficult and challenging. However, meaningful electrical characteristics can be measured by
11 employing compact highly oriented crystalline and monolithic thin films of MOFs instead,
12 which can be grown by quasi liquid phase epitaxy (LPE).^[6] Such monolithic and dense highly
13 oriented MOF thin films are referred to as surface-anchored metal-organic framework
14 (SURMOF) films. The superior elastic and mechanical properties of SURMOF films have
15 already been reported for single layered materials as well as in multilayered architectures.^[7,8]

16
17
18
19
20
21
22
23
24
25
26
27
28 Therefore, compact highly oriented SURMOF films offer a clear advantage in this context. A
29 number of different techniques and methods are currently known for preparing polycrystalline
30 MOF coatings^[9]; in addition, the deposition of MOF^[10] materials has been described for the
31 fabrication of electrical and microelectronic devices.^[11,12] It is rather obvious that the electrical
32 properties of porous MOFs/SURMOFs change when guest molecules are loaded into the pores
33 of the framework. The first studies of this type were reported by Dragässer et al, for the case of
34 loading ferrocene inside monolithic HKUST-1 SURMOF thin films^[13], where the acronym
35 HKUST denotes “Hong Kong University of Science & Technology, that originally publicized
36 this MOF structure. Later, Talin et al. found that after loading TCNQ
37 (Tetracyanoquinodimethane) molecules into the framework of HKUST-1, the electrical
38 conductivity increased over six orders of magnitude with values up to 7 S/m in air.^[14]

39
40
41
42
43
44
45
46
47
48 First models have suggested that the conductivity arises from redox-active TCNQ guest
49 molecules linking the copper paddlewheels within the open pores of HKUST-1. Charge
50 transport between the TCNQ guests has been recently described and theoretically investigated
51 by a second order process.^[15] In this experimental study, it was also pointed out that
52 inconsistencies exist between the electron-conducting mechanism proposed by these authors
53 and the experimentally established positive sign of the Seebeck-coefficient^[16], which points to
54 a *p*-type conducting mechanism.
55
56
57
58
59
60

1
2
3 Here, we investigate the electrical properties of pristine HKUST-1 and TCNQ loaded compact
4 HKUST-1 SURMOF films by I-V characteristics and four-point Van der Pauw Hall
5 configuration measurements. The compact MOF thin films were grown on pretreated Si and
6 nonconductive borosilicate and quartz substrates using quasi liquid phase epitaxy (LPE) in
7 conjunction with a spray process already reported in our previous studies.^[6] This process yields
8 film thicknesses in the range of ≈ 40 -100 nm, depending on the number of spraying cycles
9 used.^[17] SURMOF films were characterized using X-ray diffraction and IRRAS measurements.
10 Morphological studies through scanning electron microscope (SEM) cross-sectional
11 measurements have been applied to check for continuity, homogeneity, and compactness of the
12 monolithic SURMOF thin films, as well as to detect possible meso/macro porosity within the
13 quasi epitaxially grown SURMOF films. Recently, a number of alternative procedures have
14 been developed for the fabrication of MOF thin films, including dipping, spin-coating as well
15 as electrochemical techniques.^[4,17] However, it has been difficult to achieve high quality
16 oriented MOF thin films with low defect density using the above-described methods. In
17 contrast, it is possible to growth very compact and highly oriented SURMOF thin films of high
18 morphological quality and low surface roughness by employing the controlled process of quasi
19 liquid phase epitaxy (LPE) on functionalized Si/Au substrates.^[11] Excellent quality of highly
20 oriented or polycrystalline HKUST-1 thin films can be achieved on modified silicon and quartz
21 substrates, which is an essential prerequisite for enabling good electrical contacts and
22 horizontal/in-plane electrical conductivity measurements in order to obtain reproducible results.
23 SURMOF films synthesized from other metal-organic framework systems have been studied in
24 previous works with regard to their mechanical,^[7] optical/photonic,^[18] magnetic,^[19] or electrical
25 ^[20] behavior, which are key properties for the desired functionality.

26
27
28
29
30
31
32
33
34
35
36
37
38
39
40
41
42
43
44
45
46
47
48
49
50
51
52
53
54
55
56
57
58
59
60
HKUST-1 is constructed from Cu^{++} dimers and benzene-tricarboxylate (BTC) units which form
a crystalline, 3-D porous structure with a pore diameter of 1.2 nm, where the available pores
allow the loading or storage of guest molecules for example TCNQ inside the MOF structure
(see the schematic chemical model of Fig. 1 A). HKUST-1 MOF films used in this study were
grown on plasma-treated silicon and glass substrates by LPE spray method ^[9], in which the
metal-containing solution [1 mmol $\text{Cu}(\text{OAc})_2$] and the linker solution [0.1 mmol BTC] are
sprayed subsequently on the pretreated substrate. For this study, the standard spray procedure
was modified by omitting the rinsing process with pure ethanol in order to achieve random
polycrystalline, non-oriented MOF films, which is a prerequisite for horizontal/in-plane
conductivity measurements due to the observed anisotropy in highly oriented quasi epitaxial
SURMOF films.^[21,22] In an earlier report such highly oriented crystalline SUMOF film have

1
2
3 been successfully used for resistive switching between film surface and film backside electrodes
4 using aligned MOF pores for charge transport.^[11] Next to electrical charge transport in MOF
5 thin films, new developments have been recently reported for their thermal conductivity.^[23, 24]
6
7

8
9 The resulting HKUST-1 SURMOF films was verified by X-ray diffraction (XRD). A typical
10 XRD diffraction pattern is displayed in Fig. 1B (black curve). The XRD data clearly
11 demonstrate the presence of polycrystalline HKUST-1 MOF films with random orientation of
12 the individual crystallites. The experimental XRD data compare well with the simulated
13 HKUST-1 MOF powder diffraction pattern.
14
15
16

17
18 The desired MOF film thickness can be adjusted using a number of distinct LPE spray cycles;
19 e.g., 15, 25, 30 and 45 spray cycles for HKUST-1 SURMOF films resulting in a total film
20 thickness of ~40, ~60, ~70 and ~100 nm as illustrated in the SEM cross-sections of Fig.3. After
21 the quasi epitaxial growth of the MOF films, all samples were characterized using X-ray
22 diffraction (XRD) with a D8-Advance Bruker AXS diffractometer with Cu K α radiation ($\lambda =$
23 1.5418 Å) in $\theta/2\theta$ geometry equipped with a position sensitive detector. XRD data have been
24 recorded for all samples before and after loading the pores with TCNQ. Morphology studies
25 were performed using cross-sectional images with a Hitachi S 4700 FE-SEM operated at 5 kV
26 for MOF films on silicon substrates on an Al-SEM cross-section holder shown in Fig. 3 and
27 also for planar view SURMOF samples shown in Fig.4 and Fig. 5.
28
29
30
31
32
33
34
35

36
37 The loading of TCNQ into the HKUST-1 MOFs was carried out by a liquid-phase procedure,
38 where the as-synthesized MOF thin film was first activated by annealing at 60 oC for 4 h to
39 remove any remaining solvent stored in the pore of MOF materials. Subsequently, the samples
40 were immersed into an ethanolic TCNQ solution (2mM) for 72 h at room temperature. Finally,
41 the sample was rinsed using pure ethanol to remove the TCNQ molecules adsorbed on the
42 surface. To ascertain the successfully loading of TCNQ molecules, Raman spectra of the sample
43 before and after loading as well as the drop cast TCNQ molecule on a gold substrate were
44 recorded and are displayed in Fig. 1C. The Raman spectra recorded after loading provide a clear
45 signature of TCNQ molecules, such as the peak at 2221 cm⁻¹ and 1601 cm⁻¹ wavenumbers.
46 These Raman signals were assigned to the C and N triple bond stretch and C and C double bond
47 wing stretch, respectively and provide a signature for the presence of TCNQ. The other Raman-
48 bands related to the HKUST framework showed no changes after loading, which suggests that
49 the infiltration with TCNQ did not change or deteriorate the original HKUST-1 SURMOF host
50 structure. XRD data received from the sample after loading with TCNQ provided additional
51 evidence that the thin films are still crystalline. The slight change of relative XRD intensity is
52
53
54
55
56
57
58
59
60

1
2
3 attributed to the form factor change after loading the guest molecule into the porous crystal
4 structure. Fig. 2 a & b) highlights the difference between quasi-epitaxial growth of
5 preferentially oriented SURMOF films grown on quartz versus polycrystalline SURMOF films
6 grown on thermal oxidized SiO₂/Si wafer.^[24] All chemical precursors used in this work are
7 commercially available from Sigma Aldrich and the *p*-type Silicon substrates were received
8 from Silchem Handelsgesellschaft GmbH, Germany.
9

10
11
12
13
14 HKUST-1 SURMOF films were quasi liquid-phase epitaxially (LPE) grown with a preferential
15 crystal orientation on functionalized interfaces, which consisted of a thin Au film followed by a
16 self-assembled monolayer (SAM layer) on silicon wafers covered with a native oxide layer. The
17 LPE spray method has already been described elsewhere,^[4,17] where the metal-containing solution
18 [1 mmol Cu(OAc)₂] and the linker solution [0.1 mmol BTC] are sprayed alternately on the Si or
19 borosilicate substrate.
20
21
22
23
24

25
26 The desired MOF film thickness can be adjusted using a number of distinct LPE spray cycles; e.g.,
27 15, 25, 30 and 45 spray cycles for HKUST-1 SURMOF films resulting in a total film thickness of
28 ~40, ~60, ~70 and ~100 nm as illustrated in the SEM cross-sections of Fig.3. After the quasi
29 epitaxial growth of the MOF films, all samples were characterized using X-ray diffraction (XRD)
30 with a D8-Advance Bruker AXS diffractometer with Cu K α radiation ($\lambda = 1.5418 \text{ \AA}$) in $\theta/2\theta$
31 geometry equipped with a position sensitive detector. XRD data have been recorded for all samples
32 before and after loading the pores with TCNQ. Morphology studies were performed using cross-
33 sectional images with a Hitachi S 4700 FE-SEM operated at 5 kV for MOF films on silicon
34 substrates on an Al-SEM cross-section holder shown in Fig. 3 and also for planar view SURMOF
35 samples shown in Fig.4 and Fig. 5.
36
37
38
39
40
41
42

43 ***Electrical Measurements***

44 **Seebeck Coefficient**

45
46 To elucidate the electrical characteristics of SURMOF films we conducted Seebeck coefficient
47 measurements, Current-Voltage (I-V) characteristics and Van der Pauw four-point Hall
48 configuration measurements. First, we measured the Seebeck coefficient *S* as a function of
49 temperature for random polycrystalline SURMOF films infiltrated with TCNQ and compared the
50 results with the case of preferentially (001) orientated SURMOF films with TCNQ loading,
51 referred to in the XRD plots of Fig 2b. During our Seebeck measurements of dense highly oriented
52 crystalline SURMOF films a strong anisotropy of electrical conduction was observed between
53 preferentially oriented quasi liquid epitaxial SURMOF films versus random polycrystalline MOF
54
55
56
57
58
59
60

1
2
3 films. Fig. 6a plots the temperature dependence of the measured Seebeck coefficient of quasi-
4 epitaxial highly oriented SURMOF films with and without (pristine) TCNQ infiltration. In both
5 cases for pristine and loaded MOFs, the horizontal Seebeck coefficient of highly oriented
6 SURMOF films is hardly measurable fluctuating around $0 \mu\text{V/K}$ and in the noise level over the
7 entire temperature testing range from 295 K to 350 K. However, for the case of random
8 polycrystalline SURMOF films grown on thermal oxidized Si substrates with thick 484 nm
9 isolation SiO_2 the horizontal Seebeck coefficient is measurable over the temperature range between
10 290 K and 350 K. The maximum measured Seebeck coefficient of TCNQ loaded polycrystalline
11 MOFs with film thickness of 200 nm and TCNQ infiltration was $422.32 \mu\text{V/K}$ at 350 K, see Fig.6b.
12 We attribute these results to the fact that SURMOF films grown on SAM functionalized gold
13 coated Si substrates exhibit a strong preferential orientation along the (001) direction.^[4] For such
14 highly preferentially oriented films a previous study has demonstrated good charge carrier
15 transport only through the vertical direction with surface top contacts and backside contacts^[11]
16 while no carrier transport takes place in the horizontal in-plane direction parallel to the surface.
17 MOF films grown directly on thermally oxidized Si substrates without the use of SAM
18 functionalized Au layers are subject to heterogeneous nucleation resulting into random
19 polycrystalline MOF films. The isotropic nature of these random polycrystalline MOF films
20 enabled charge carrier transport via all directions. For this reason, the measured horizontal Seebeck
21 coefficient of highly oriented SURMOF films parallel to the surface was negligibly small around
22 $0 \mu\text{V/K}$, while the Seebeck coefficient of random oriented polycrystalline MOF films measured
23 fairly high values. It is noteworthy to point out that the measured Seebeck coefficient of
24 polycrystalline SURMOF films was positive, thereby indicating the SURMOF films are p-type,
25 where the majority charge carriers are holes. Our measurements are consistent with literature work
26 ^[16]. The positive Seebeck coefficient of TCNQ loaded polycrystalline MOF films increases linearly
27 from $342.39 \mu\text{V/K}$ to $422.32 \mu\text{V/K}$ as the temperature rises from 290 K to 350 K, because thermal
28 activation generates more charge carriers contributing to the Seebeck coefficient at higher
29 temperatures. The plots of the temperature dependent Seebeck coefficient of the pristine MOF
30 films versus the TCNQ loaded films exhibit roughly the same slope and tendency over the
31 temperature range between 290 K and 330 K and are parallel shifted by approximately $50 \mu\text{V/K}$.
32 The Seebeck coefficient S is inversely proportional to electrical conductivity σ and charge carrier
33 density n . This explains why the higher electrical conductivity of TCNQ loaded SURMOF samples
34 results necessarily in lower Seebeck coefficient values. The Mott relationship stipulates that the
35 lower carrier density of pristine undoped polycrystalline MOF films results in higher Seebeck
36 coefficients, while conversely the TCNQ loading of the pores effectively enhances the charge
37
38
39
40
41
42
43
44
45
46
47
48
49
50
51
52
53
54
55
56
57
58
59
60

1
2
3 carrier density and electrical conductivity of isotropic polycrystalline MOF films. Because of the
4 inverse relationship with carrier density this fact leads to a lower Seebeck coefficient.
5
6

7 **Thin-Film Electrical Conductometry**

8
9

10 For further investigation of the electrical properties of SURMOF films, the I-V-characteristic
11 curves of preferentially (001) oriented MOFs grown on Au and SAM functionalized Si substrate
12 or on quartz were measured and compared to polycrystalline MOFs grown on native oxide covered
13 Si substrates and on borosilicate glass.
14
15

16 All the electrical properties measurements were performed with an Ecopia Hall effect measurement
17 system (HMS-5300) using a symmetrical four-point Van der Pauw Hall configuration sample ²⁵.
18 The Hall system is equipped with a 0.556 T permanent magnet, and a variable temperature test is
19 available from 80 K to 550 K. Liquid nitrogen was used to cool down the system to the desired
20 initial test temperature. In the experiment, square-shaped samples in size of 1 cm × 1 cm with four
21 symmetrical Au surface contacts on the corners were prepared for testing. Initially, for the first set
22 of electrical tests the Au electrodes were sputter deposited directly on the surface of the MOF film
23 on the four corners of the sample through use of a shadow mask in a Van der Pauw sample
24 arrangement. The four Au surface contacts were of equal size and less than 1 × 1 mm² in area and
25 with a thickness of 150 nm. Fig. 7b displays a photographic image of the Hall measurement stage
26 mounted a sample with the four sputtered Au contacts using a Van der Pauw Hall configuration
27 sample. However, ongoing analysis revealed that any surface Au contacts fabricated by either
28 sputtering, thermal evaporation or e-beam evaporation causes deterioration of the hybrid SURMOF
29 material and physical surface damage complicating the evaluation of test results. For this reason,
30 we resorted to bottom Au contacts. For this endeavor we designed a shadow mask for square
31 samples, which allows to sputter the Au contacts through the mask openings to fabricate the four
32 corner bottom contacts. This way we made sure to protect the physical integrity of the SURMOF
33 films by always using bottom Au contacts with a mask and subsequently synthesized the SURMOF
34 films on top of the pre-deposited gold contacts. These protective measures ensure a pristine
35 condition of the surface morphology and integrity of the SURMOF films. Fig. 7a provides a
36 schematic of the sample stage pre-structured with four bottom Au contacts illustrating the design
37 of the test sample, while Fig. 7b provides a photographic image of the Hall Effect measurement
38 stage with square SURMOF sample with sputtered Au bottom contacts in the four corners for a
39 Van der Pauw configuration. The characteristic I-V curves of polycrystalline SURMOF films on
40 borosilicate glass substrates with and without TCNQ infiltration are displayed in the plots of Fig.
41 8. The measurements demonstrate that the TCNQ loading is boosting lateral electrical conductivity
42
43
44
45
46
47
48
49
50
51
52
53
54
55
56
57
58
59
60

1
2
3 in the film and results in a measurable I-V curve, while the pristine non-loaded MOF films exhibit
4 practically zero conductivity. Lateral in-plane Current-Voltage measurements were conducted on
5 the Van der Pauw samples between two Au contacts and were repeated for the following contact
6 pairs: AB, BC, CD and between contacts DA. Clearly the TCNQ infiltration helps the SURMOF
7 films on borosilicate glass to attain a meaningful conductivity, and the linear I-V curve indicates
8 good Ohmic conduction. For comparison and in stark contrast, the I-V curve of preferentially (001)
9 oriented MOF films grown on quartz substrates reveal in Fig. 9, that TCNQ loading with the
10 concomitant increase in carrier density cannot affect any horizontal in-plane electrical conduction
11 for the case of all preferentially oriented SURMOF films. Both TCNQ loaded and pristine
12 SURMOF films show lateral in-plane current of zero measured in the voltage range from -10 V to
13 10 V. These results corroborate the Seebeck results and further demonstrate that these
14 preferentially (001) oriented SURMOF films exhibit a large electrical anisotropy with no charge
15 carrier transport in the horizontal direction parallel to the sample surface, but only carrier transport
16 in the vertical direction from front to backside, where switching effects have been reported.^[11] The
17 SURMOF films grown on borosilicate glass without any surface functionalization produce random
18 polycrystalline films that allow the majority charge carrier hole transport horizontally through the
19 film between two contacts, because the randomness ensures sufficient numbers of grains with the
20 crystallographic orientation that conduct electrical current.

21
22 In order to further confirm the accuracy and reproducibility of the four-point Van der Pauw
23 measurements a new set of SURMOF films were subsequently synthesized on hydroxyl terminated
24 native oxide covered Si substrates in the same way as the ones studied in the previous section and
25 the texture and morphology was compared with the films grown on borosilicate glass substrates.
26 Fig. 4 displays planar view FE-SEM micrographs of MOF films grown on borosilicate glass
27 substrates showing pristine MOFs and TCNQ loaded MOFs of 10 cycles and 40 cycles resulting
28 in thickness of ~40 nm and ~130 nm. However, the MOF films grown on borosilicate glass
29 substrate exhibit a loosely stacked granular surface morphology with considerable gaps between
30 the individual MOF grains. The MOF film morphology obtained on borosilicate glass substrates
31 is in contrast with the more dense and compact SURMOF films grown on hydroxyl terminated
32 native oxide covered silicon substrates, shown in Fig. 5, where all the MOF grains are in direct
33 physical contact forming a continuous compact film thereby creating a good electrical connection
34 shown in Fig. 11. This morphological difference is attributed to the lack of proper surface wetting
35 by lacking hydroxyl surface termination and inferior chemisorption of the LPE sprayed MOF film
36 on borosilicate glass.

1
2
3 The investigation of the temperature dependence of the electrical conductivity σ of random
4 polycrystalline MOF films of ~ 130 nm thickness grown on insulating borosilicate glass substrates
5 in the temperature range of 260 \sim 350 K is shown in the plot of Fig. 10a. The electrical conductivity
6 σ increases as a function of rising temperature, which is attributed to thermal activation generating
7 more majority charge carriers in the SURMOF film. Interestingly, this temperature dependent
8 electrical conductivity behavior indicates semiconductor-like conductivity as opposed to metal
9 conductivity behavior. As temperature increases from 260 K to 350 K, the electrical conductivity
10 of TCNQ loaded MOF increases from 7.129×10^{-4} S/cm to 3.1×10^{-3} S/cm. The results are
11 consistent with reported works.^[15,16] The low electrical conductivity of MOF films grown on
12 borosilicate glass substrates results from the activation energy of the sample, which can be
13 calculated from the slope of $\sigma(T)$ vs. $1/T$ curve shown in Fig.10b based on $\sigma \sim \exp(E_a/T)$. The
14 red line represents a linear fit that represents a thermally activated process where the sample shows
15 a near-linearly relationship between electrical conductivity and the reciprocal of temperature over
16 temperature range of 300 K \sim 350 K with an activation energy E_a of 0.13 eV, which is above
17 reported values of 0.052 eV.^[15] For benchmarking the electrical conductivity over the temperature
18 range of 260 \sim 350 K of polycrystalline SURMOF films grown on 40 nm thick thermal isolating
19 SiO_2 covered Si substrates with bottom Au contacts has been plotted in Fig. 11a. In Fig. 9b the red
20 line is linear fit that represents a thermally activated process with an activation energy of 0.043 eV.
21 The slope of the Arrhenius plot can be expressed as E_a/k , where E_a represents activation energy,
22 and k is Boltzmann constant. A low activation energy generally is indicative of a higher charge
23 carrier density and hence higher electrical conductivity. The activation energy E_a of SURMOF
24 films grown on thick amorphous isolating SiO_2 on Si substrates is smaller compared to the
25 SURMOF films grown on borosilicate glasses, indicating the SURMOF films grown on SiO_2/Si
26 substrates exhibit a higher electrical conductivity. This is attributed to morphological differences
27 between relatively loosely stacked and more porous SURMOF films grown on borosilicate glass
28 versus compact and dense MOF films grown on hydroxyl terminated SiO_2 interfaces on Si
29 substrates highlighted in the SEM micrographs of Fig. 4 and Fig. 5. The chemistry of the growth
30 interface exerts a considerable influence on the resulting morphology of SURMOF HKUST-1 film
31 by providing better chemisorption and better surface wetting of the precursor chemicals resulting
32 in saturated nucleation sites. In a separate study C. Wilmer et al. demonstrated that infiltration of
33 the pores in SURMOF films with absorbates also affects thermal transport by introducing
34 additional phonon scattering in HKUST-1 SURMOF films thereby greatly lowering thermal
35 diffusivity and reducing thermal conductivity in HKUST-1 films.^[25]

1
2
3 Recent advances in another MOF category of e.g. layered $\text{Ni}_3(2,3,6,7,10,11\text{-hexaimino-}$
4 $\text{triphenylene})_2$ ($\text{Ni}_3(\text{HITP})_2$)^[26] MOGs (Molecular-Organic Graphene) report significant increases
5 in electrical conductivity, which looks promising for future reliable Hall analysis.
6
7

8
9 Furthermore, we attempted first Hall Effect measurements in the temperature range of 260 K to
10 350 K in order to establish the critical electrical parameters like Hall coefficient, the Hall mobility
11 and the carrier density to complete a comprehensive electrical characterization of HKUST-1
12 SURMOF films. The generally positive Hall coefficient of all investigated MOF films indicate,
13 that the MOF films are p-type and the positive charge carriers are holes, which is consistent with
14 previous work^[26] and thus provides an independent confirmation of our Seebeck results on the
15 carrier type. In spite of electrical conductivities of $\sim 3.1 \times 10^{-3}$ S/cm at 350 K in SURMOF films
16 on borosilicate substrates, the contact resistances of our HKUST-1 samples were measured in
17 excess of 1 – 2 M Ω , which prevent reliable Hall measurements at a magnetic field of 0.55 Tesla.
18 Subsequently the Hall measurements were repeated at an external lab in much higher magnetic
19 fields from 1 T to 6 T using a PPMS Quantum Design Physical Property Measurement System.^[27]
20 However even at a magnetic field of 6 Tesla the MOhm contact resistant between the bottom Au
21 contacts and HKUST-1 SURMOF film proved too high for reproducible Hall measurements.^[28]
22 As future outlook and perspective, we have to summarize that the current generation of TCNQ
23 loaded HKUST-1 requires better contact technology and much improved doping techniques to
24 achieve lower contact resistances in order to enable reproducible Hall measurements.
25
26
27
28
29
30
31
32
33
34
35
36

37 In this context, Maissa Barr, J. Bachmann et al. at Friedrich-Alexander Universität Erlangen-
38 Nürnberg, Germany, have recently shown a promising new approach of achieving for the first time
39 solution-based Atomic Layer Deposition (s-ALD)^[29] synthesis of Cu-BDC MOF films, which
40 could offer in the future hitherto totally unknown technical possibilities of in-situ doping of
41 growing MOF films. As a perspective such successful demonstration of Solution based ALD (s-
42 ALD) technology of crystalline MOF films opens up the prospect of precise Angstrom film
43 thickness control of true conformal layer-by-layer growth of MOF films with superior control of
44 smooth surface morphology, which is a prerequisite for large volume industrial scale technological
45 applications ranging from sensors, batteries, fuel cells and photovoltaic devices as well as to
46 functional thin film materials in the field of electrochemistry, optoelectronics, luminescence, up-
47 conversion, proton conductivity, optics and photonics, thermoelectrics, sensing, magnetism, non-
48 linear optics, data storage as well as to photo-/electrocatalysis, membranes, chemical reactors and
49 gas storage.
50
51
52
53
54
55
56
57
58
59
60

Summary

In conclusion, we report experimentally determined electrical characterization to demonstrate different electrical properties for pristine HKUST-1 and TCNQ loaded HKUST-1 SURMOF films while benchmarking compact random polycrystalline SURMOF films versus preferentially (001) oriented films grown by the LPE spray method. In addition, the electrical conductivity as well as the Seebeck Coefficient has been investigated in detail. In our study HKUST-1 MOF thin films have been grown using liquid phase epitaxy (LPE) on surface functionalized and modified silicon and on borosilicate glass substrates. MOF thin films have been further doped with TCNQ molecules. Pristine and TCNQ loaded samples of monolithic HKUST-1 SURMOF thin films with a thickness of ~ 130 nm has been carefully investigated by Seebeck analysis and current -voltage (I-V) measurements. Our investigation has established that preferentially (001) oriented crystalline SURMOF films reveal crystal orientation dependent anisotropic electrical conductivity. Such (001) preferentially oriented crystalline SURMOF films exhibit only vertical electrical conduction between front and backside contacts of the SURMOF film, whereas there is no measurable horizontal in-plane conductivity between either two or four surface contacts. However, very dense compact and isotropic random polycrystalline MOF films have demonstrated surprisingly high in-plane electrical conductivity between van der Pauw sample surface contacts.

These fundamental Van der Pauw sample configuration measurements provide important insights into the anisotropy of electrical conduction and electrical characteristics of these materials, which renders these MOF films attractive for upcoming microelectronic and optoelectronic applications. It is foreseeable that the anisotropy of the electrical conductivity in crystalline SURMOF films lends itself readily to be advantageously exploited for electronic applications. At the current stage of materials development, the contact resistance of HKUST-1 SURMOF films are still too high to render reproducible Hall measurements feasible for a comprehensive electrical characterization. In perspective, more work in this stimulating field is required. In particular, the doping technology of SURMOF films must be improved dramatically to increase the carrier density and electrical conductivity and to improve the contact resistance.

There is no fundamental roadblock to prevent further steady materials improvement as this materials class possesses outstanding and tunable electrical properties for highly conductive SURMOF thin film materials and coatings. Based on this initial electrical characterization work we anticipate a promising future of SURMOF films with good potential in the future initially in thermoelectric applications and with improved electrical conductivity later on in microelectronic systems applications.

Acknowledgments

E.R. is thanking the DFG, KIT and CMM for sustainable research funding. This work was funded within the priority program SPP 1362 and SPP 1928 of the German Research Foundation (DFG). The authors would like to acknowledge the College of William and Mary (Williamsburg, Virginia) for the use of the FE-SEM and California State University Los Angeles for the Quantum Design PPMS experiments.

REFERENCES

- [1] a) E. G. Bittle, J. I. Basham, T. N. Jackson, O. D. Jurchescu, D. J. Gundlach, *Nature Commun.* **7**, 10908 (2016); b) S. Hunter, J. W. Ward, M. M. Payne, J. E. Anthony, O. D. Jurchescu, T. D. Anthopoulos, *Appl. Phys. Lett.* **106**, 223304 (2015)
- [2] a) H. Li, M. Eddaoudi, M. O'Keeffe, and O. M. Yaghi, *Nature* **402** (6759), 276-279 (1999)
b) O. M. Yaghi, G. M. Li, and H. L. Li, *Nature* **378** (6558), 703-706 (1995)
- [3] G. Ferey and C. Serre, *Chem. Soc. Rev.* **38** (5), 1380-1399 (2009)
- [4] O. Shekhah, J. Liu, R. A. Fischer and Ch. Wöll, *Chem. Soc. Rev.*, **40**, 1081-1106 (2011)
- [5] J. Liu, B. Lukose, O. Shekhah, H. K. Arslan, P. Weidler, H. Gliemann, S. Bräse, S. Grosjean, A. Godt, X. Feng, K. Müllen, I.-B. Magdau, T. Heine and Ch. Wöll, *Sci. Rep.* **2**, 921, (2012)
- [6] O. Shekhah, H. Wang, S. Kowarik, F. Schreiber, M. Paulus, M. Tolan, C. Sternemann, F. Evers, D. Zacher, R. A. Fischer, Ch. Wöll, *J. Am. Chem. Soc.* **129**, 15118 (2007)
- [7] S. Bundschuh, O. Kraft, H. K. Arslan, H. Gliemann, P. G. Weidler and Ch. Wöll, *Appl. Phys. Lett.* **101**, 101910 (2012)
- [8] J. P. Best, J. Michler, J. Liu, Z. Wang, M. Tsotsalás, X. Maeder, S. Roese, V. Oberst, J. Liu, S. Walheim, H. Gliemann, P. G. Weidler, E. Redel and C. Wöll, *Appl. Phys. Lett.* **107**, 101902 (2015)
- [9] a) S. Hermes, F. Schroder, R. Chelmoski, Ch. Wöll and R. A. Fischer, *J. Am. Chem. Soc.*, **127** (40), 13744–13745 (2012)
b) E. Biemmi, C. Scherb and T. Bein, *J. Am. Chem. Soc.*, **129** (26), 8054 - 8055 (2007)
c) P. Horcajada, C. Serre, D. Grosso, C. Boissiere, S. Perruchas, C. Sanchez, G. Ferey, *Advanced Mater.*, **21**(19), 1931-1935 (2009)
- [10] H. Gliemann and Ch. Wöll, *Materials Today* **15** (3), 110-116 (2012)
- [11] Z. Wang, D. Nminibapiel, P. Shrestha, J. Liu, K. P. Cheung, W. Guo, P. G. Weidler, H. Baumgart, C. Wöll, *E. Redel ChemNanoMat* **2** (1), 67-73 (2016)
- [12] S. M. Yoon, S. C. Warren, B. A. Grzybowski, *Angew. Chem. Int. Ed.* **53**, 4437-4441(2014)
- [13] A. Dragässer, O. Shekhah, O. Zybalyo, C. Shen, M. Buck, C. Wöll, D. Schlettwein, *Chem. Communication* **48**, 663 - 665 (2012)
- [14] A.A. Talin, A. Centrone, A.C. Ford, M.E. Forster, V. Stavila, P. Haney, R.A. Kinney, V. Szalai, F.E. Gabaly, H.P. Yoon, F. Léonard, M.D. Allendorf, *Science*, **343**, 66 (2014)
- [15] T. Neumann, J. Liu, T. Wächter, P. Friederich, F. Symalla, A. Welle, V. Mugnaini, V. Meded, M. Zharnikov, C. Wöll, W. Wenzel *ACS Nano*, **10** (7), 7085-93 (2016)
- [16] K. J. Erickson, F. Léonard, V. Stavila, M. F. Foster, C. D. Spataru, R. E. Jones, B. M. Foley, P. E. Hopkins, M.D. Allendorf, A.A. Talin, *Adv. Mater.* **27**, 3453-3459 (2015)
- [17] H. K. Arslan, O. Shekhah, J. Wohlgemuth, M. Franzreb, R. A. Fischer, Ch. Wöll, *Adv. Funct. Mater.* **21**, 4228-4231 (2011)
- [18] J. Liu, E. Redel, Z. Wang, V. Oberst, J. Liu, S. Wahlheim, S. Heissler, M. Bruns, H. Gliemann, C. Wöll *Chem. Mater.* **27**, 1991-1996 (2015)
- [19] M. E. Silvestre, M. Franzreb, P. G. Weidler, O. Shekhah and Ch. Wöll, *Adv. Funct. Mater.* **23**, 1210-1213 (2013)
- [20] Xing Huang, Peng Sheng, Zeyi Tu, Fengjiao Zhang, Junhua Wang, Hua Geng, Ye Zou, Chong-an Di, Yuanping Yi, Yimeng Sun, Wei Xu and Daoben Zhu, *Nature Communications* **6**, 7408 (2015)
- [21] Xin Chen, X.; Wang, Z.; Lin, P.; Zhang, K.; Baumgart, H.; Redel, E.; Wöll, C. *ECS Trans.*, **75**, 119–126, (2016)

- 1
2
3
4 [22] Xin Chen, Zhengbang Wang, Zeinab Mohamed Hassan, Pengtao Lin, Kai Zhang, Helmut Baumgart,
5 and Engelbert Redel, *ECS Journal of Solid-State Science and Technology*, **6** (4), P150-P153 (2017)
6 [23] Engelbert Redel and Helmut Baumgart, *APL Materials* **8**, 060902 (2020)
7 [24] H. Babaei, M. E. DeCoster, M. Jeong, Z. M. Hassan, T. Islamoglu, H. Baumgart, A. J. H. McGaughey,
8 E. Redel, O. K. Farha, P. E. Hopkins, J. A. Malen, C. E. Wilmer, *Nature Communication*,
9 doi.org/10.1038/s41467-020-17822-0 (2020)
10 [25] L. J. Van der Pauw, **20** (8), 220–224 (1958)
11 [26] a) L. Sun, B. Liao, D. Sheberla, D. Kraemer, J. Zhou, E. A. Stach, D. Zakharov, V. Stavila, A. A.
12 Talin, Y. Ge, M. D. Allendorf, G. Chen, F. Leonard, M. Dincă, *Joule* **1**, 167 (2017); b) L. Sun, M. G.
13 Campbell, M. Dincă, *Angew. Chemie Int. Ed.*, **55**, 3566-3579 (2016)
14 [27] Bo Truong and Guo-Meng Zhao, Private Communication, MOF Hall Coefficient Measurements using
15 Quantum Design PPMS, Department of Physics and Astronomy, California State University, Los
16 Angeles, USA (2019)
17 [28] Chen, X., Dissertation, Old Dominion University: Norfolk, Virginia, (2017)
18 [29] M. K. S. Barr, S. Nadiri, D.H. Chen, P. G. Weidler, H. Baumgart, E. Redel, C. Asker, K. Forberich, F.
19 Hoga, T. Stubhan, H. Egelhaaf, C. Brabec, and J. Bachmann, *Atomic Layer Deposition from Dissolved*
20 *Precursors -‘Solution ALD’ (sALD)*, Abstract Nr. H05- 142750, 2nd International Symposium H05:
21 *Metal Organic Frameworks (MOFs), Covalent Organic Frameworks (COFs) and Porous Hybrid*
22 *Materials: Characterization, Technology, Bio-Applications, and Emerging Devices*
23 *at the ECS PRiME 2020 Fall Meeting of the Electrochemical Society, Honolulu, Hawaii (2020)*
24
25
26
27
28
29
30
31
32
33
34
35
36
37
38
39
40
41
42
43
44
45
46
47
48
49
50
51
52
53
54
55
56
57
58
59
60

Figures

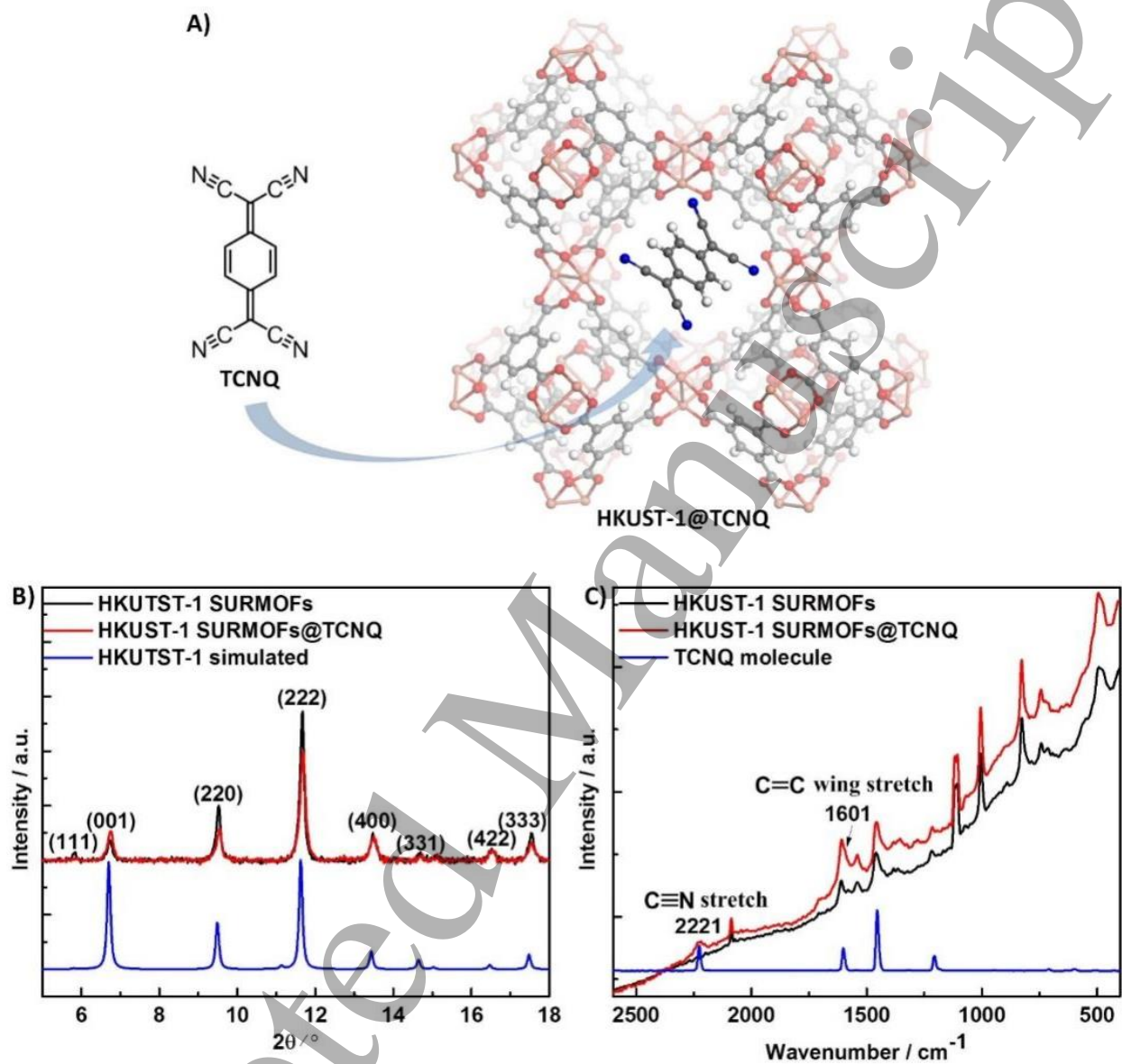


Fig. 1 (A) Schematic illustration depicting the structure of HKUST-1 SURMOF films, where the pores are loaded with TCNQ (TCNQ, tetracyanoquinodimethane). (B) plot of X-ray diffraction (XRD) patterns of pristine random polycrystalline HKUST-1 SURMOF films shown in black, while the experimental data of the HKUST-1 SURMOF films loaded with TCNQ are plotted in red. For comparison, a simulated HKUST powder diffraction plot is shown in blue color. It is apparent that the loading of the HKUST-1 pores with TCNQ did not alter or disturb the crystal structure. (C) Plot of Raman spectrum of pristine HKUST-1 SURMOF films versus the HKUST-1 SURMOF films loaded with TCNQ in the pores, Ref.^[23]

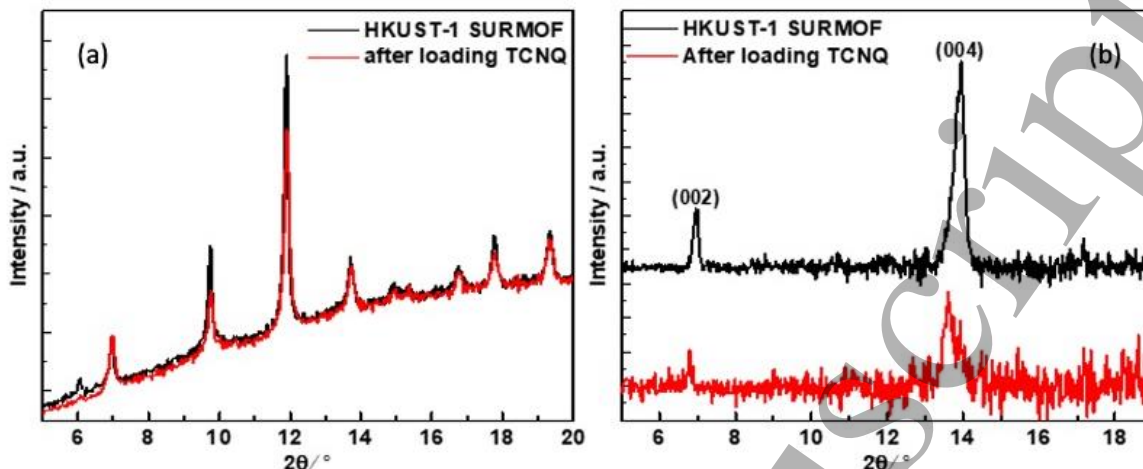


Fig. 2 XRD plots highlighting the difference between quasi epitaxial growth of preferentially oriented SURMOF film versus polycrystalline XRD signature, (a) random polycrystalline HKUST-1 SURMOF films before (black line) and after (red line) TCNQ loading grown on thermal oxidized SiO_2/Si wafer, (b) preferentially (001) oriented crystalline HKUST-1 SURMOF films before (black line) and after (red line) TCNQ loading obtained by growth on SAMs functionalized Au surface or on quartz. With permission from Ref.^[22]

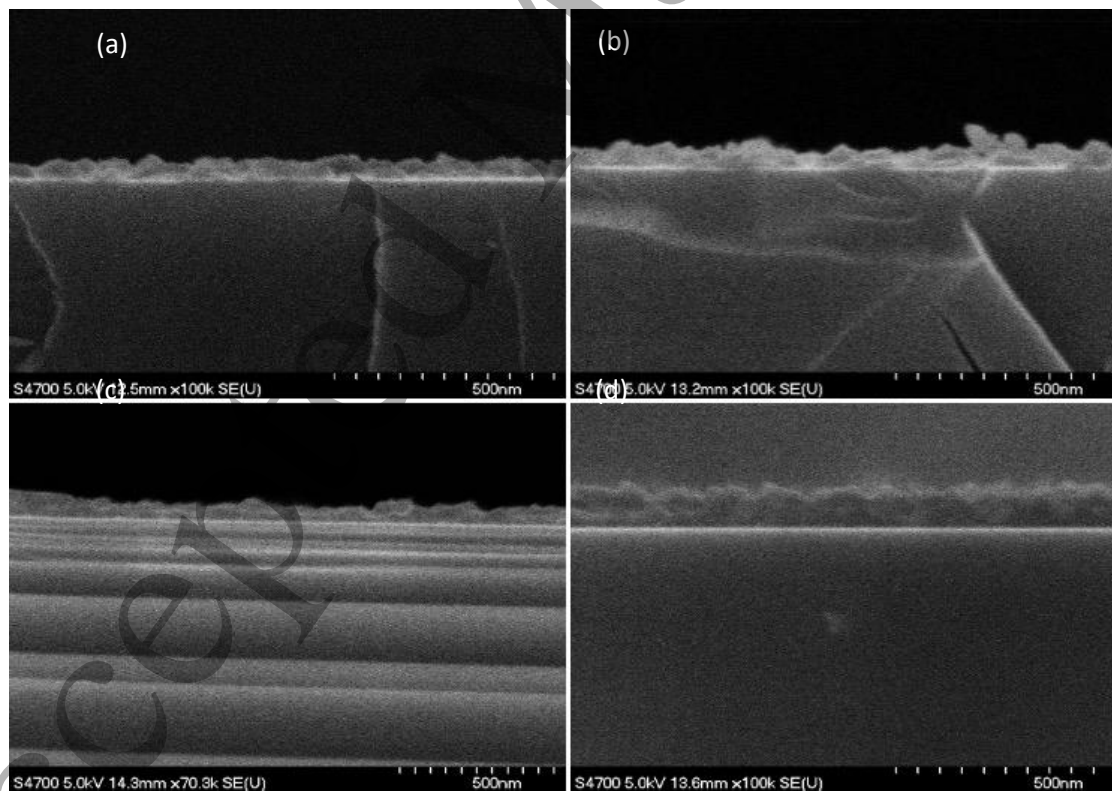


Fig. 3 FE-SEM cross-sectional micrographs of SURMOF HKUST-1 films with thickness of (a) 40 nm, (b) 60 nm, (c) 70 nm, and (d) 100 nm on Silicon substrates. Ref.^[23,28]

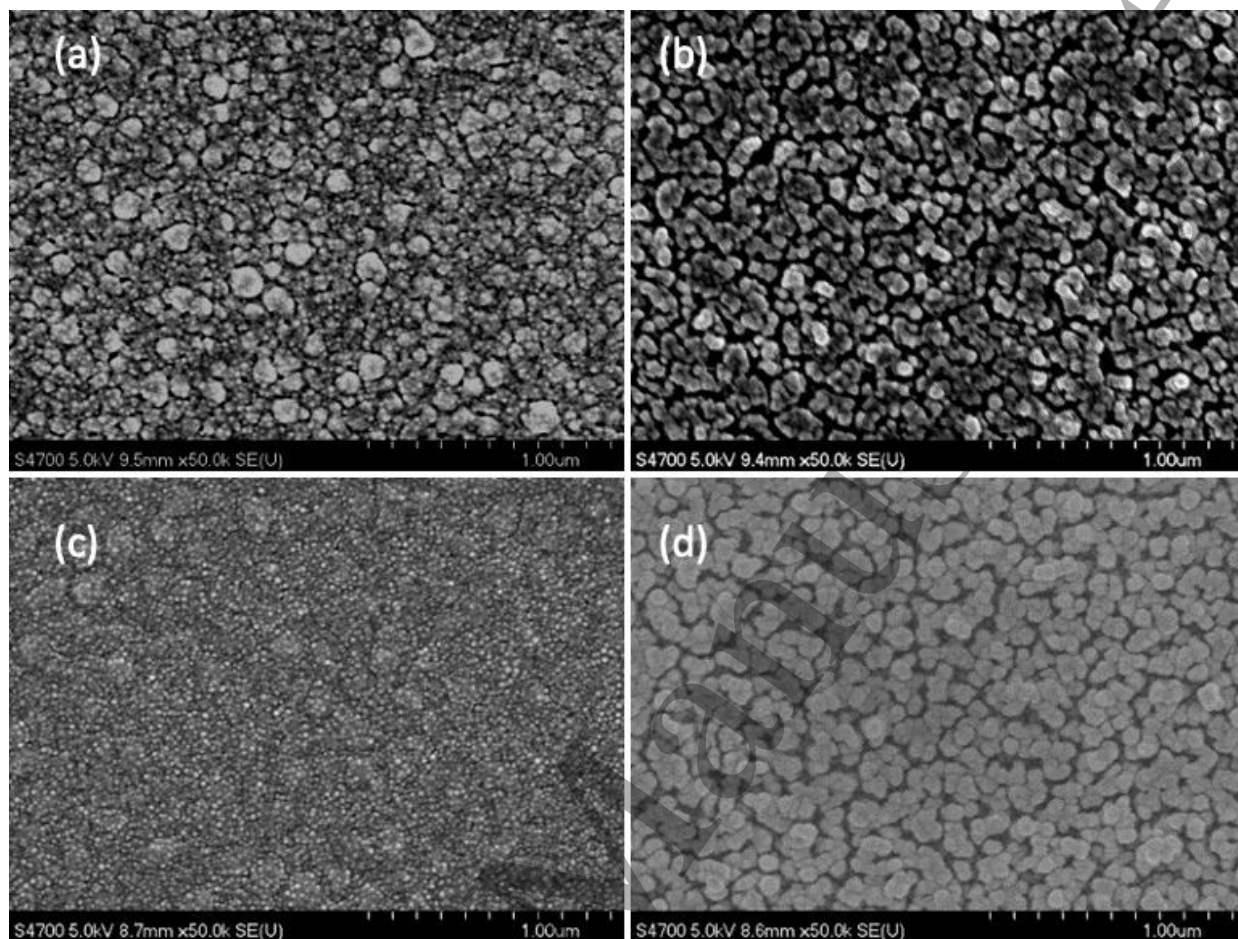


Fig. 4 Planar view FE-SEM micrographs of MOF films grown on borosilicate glass substrates displaying a different MOF morphology of very loosely stacked MOF grains with very noticeable gaps between individual MOF grains (a) 10 cycles pristine MOF (b) 10 cycles TCNQ loaded MOF (c) 40 cycles MOF pristine (d) 40 cycles MOF with TCNQ loading

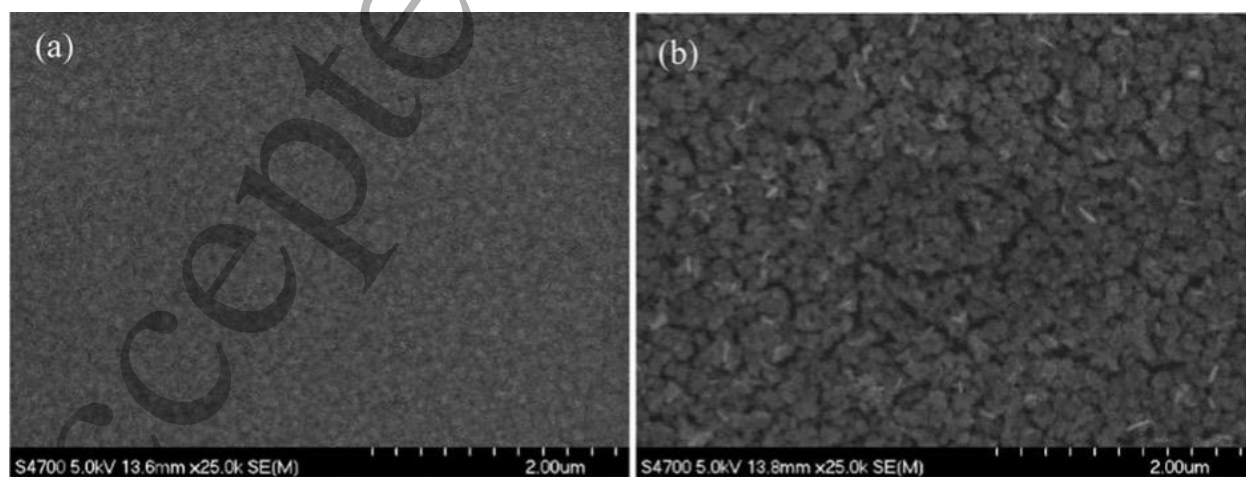


Fig. 5 Top-down planar view FE-SEM micrographs of (a) pristine and (b) TCNQ loaded random polycrystalline SURMOF HKUST-1 thin film synthesized on hydroxyl terminated SiO_2/Si substrate.

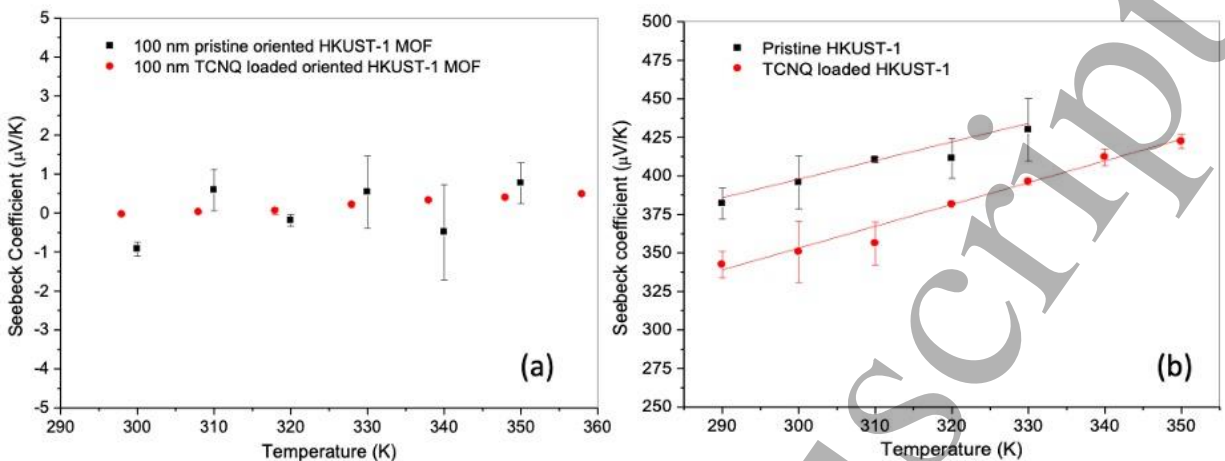


Fig. 6 (a) Seebeck coefficient measurements as function of temperature of LPE highly oriented HKUST-1 films with a thickness of 100 nm, which were prepared with and without TCNQ loading. For the case of the highly oriented SURMOF film the Seebeck coefficient oscillates around zero within the margin of error (b) However, in the case of random polycrystalline SURMOF films the Seebeck coefficient is measurable and increases as a function of temperature of LPE polycrystalline HKUST-1 thin film with a thickness of 200 nm. Pristine HKUST-1 SURMOF films exhibit a higher Seebeck coefficient compared to TCNQ loaded samples, Ref.^[23,28]

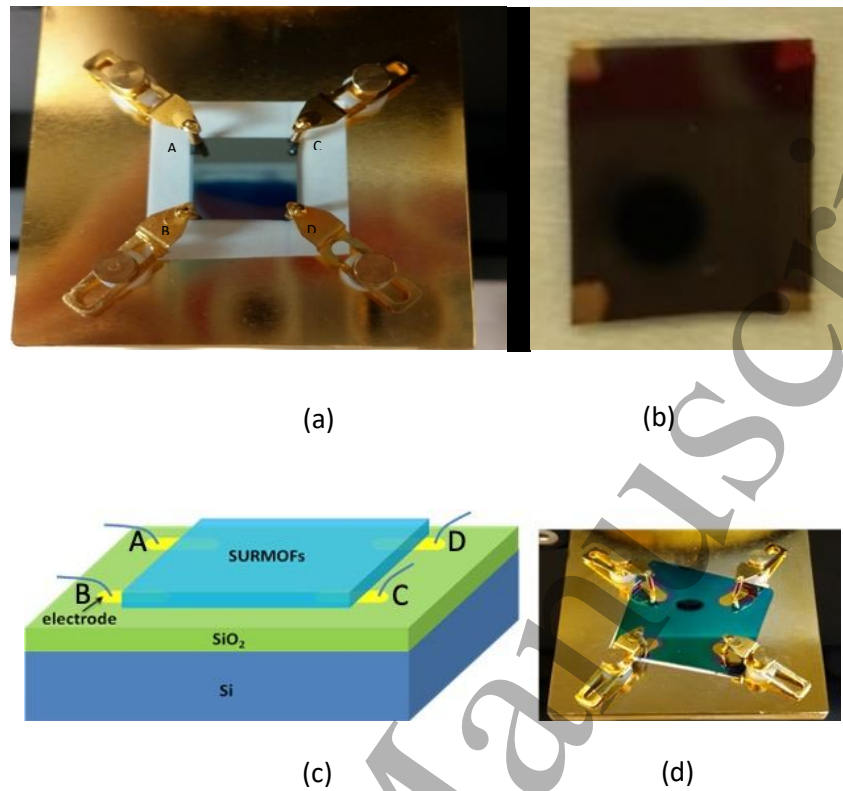


Fig. 7 (a) Photographic image of Hall sample measurement stage showing the mounted test device. (b) Photograph image of a square SURMOF sample with sputtered Au contacts on the surface of the MOF film in the four corners for a Van der Pauw Hall sample configuration. (c) Schematic of the MOF samples with four bottom contacts. (d) Hall Effect measurement stage with square MOF sample with sputtered Au bottom contacts in the four corners for a Van der Pauw configuration, Ref.^[28]

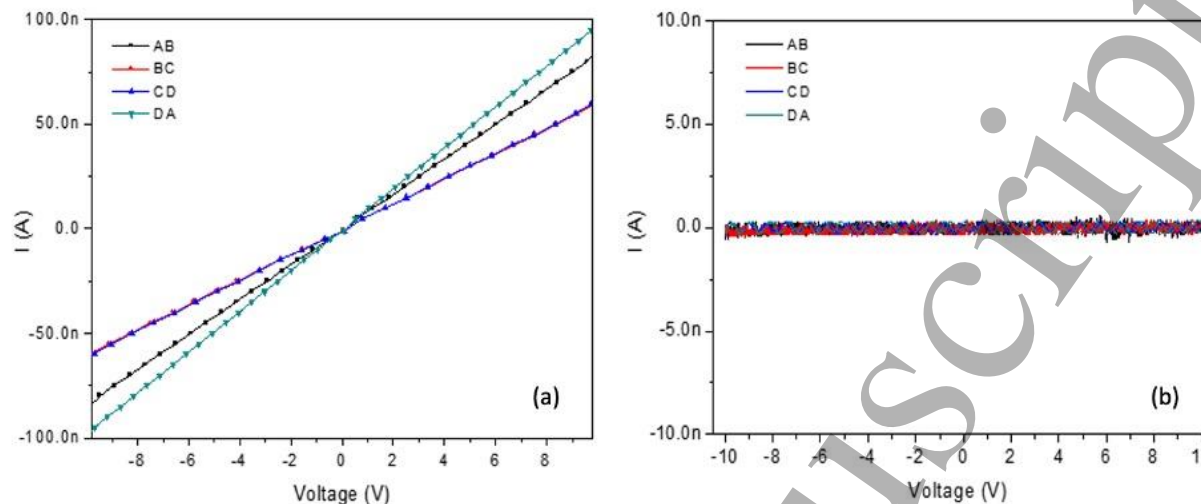


Fig. 8 (a) Plot of I-V characteristics of TCNQ loaded random polycrystalline SURMOF films grown on insulating borosilicate glass. (b) I-V characteristic of pristine random polycrystalline SURMOF film grown on borosilicate glass. Infiltration with TCNQ molecules and the concomitant increase in carrier density greatly improves the lateral in-plane electrical conductivity of polycrystalline SURMOF films. In both cases the borosilicate glass substrates were not functionalized with Au and SAMS and therefore resulted in random polycrystalline MOF films. However, only the TCNQ loaded SURMOF films with higher carrier density grown on glass produce random polycrystalline films that allow the majority charge carrier hole transport through any directions, Ref.^[28]

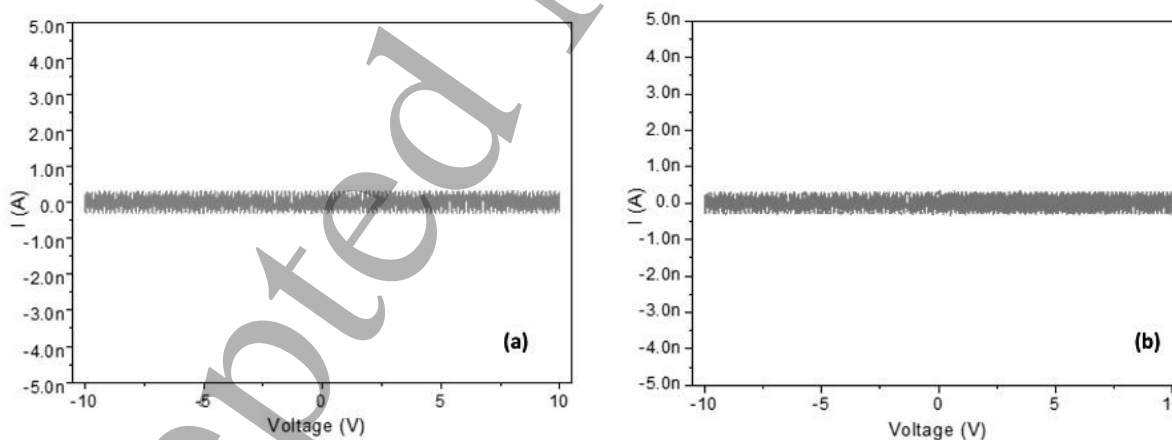


Fig. 9 (a) Plot of I-V characteristics of preferentially (001) oriented pristine (undoped) MOF films grown on surface functionalized quartz. (b) I-V characteristic of preferentially oriented SURMOF films grown on functionalized quartz substrates and loaded with TCNQ resulting in increased carrier density. Basically, there is no difference in lateral in-plane electrical conductivity between pristine and TCNQ loaded MOF samples, when the MOF films are preferentially oriented. In both cases there is no measurable lateral in-plane current, because of crystal orientation dependence of electrical conduction, Ref.^[28]

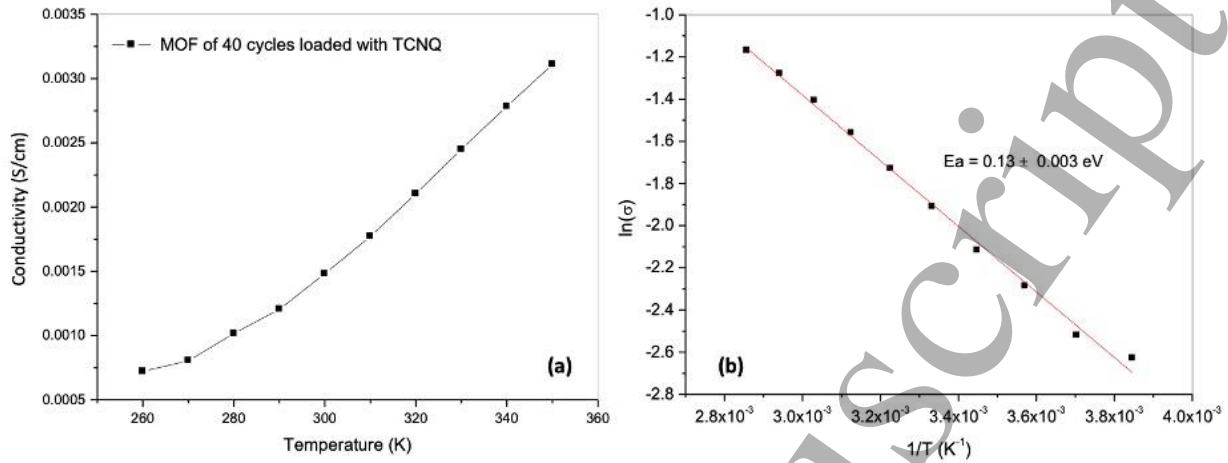


Fig. 10 (a) Plot of Temperature dependence of electrical conductivity σ of TCNQ loaded MOF grown on borosilicate glass substrate. (b) Arrhenius plot of $\ln(\sigma(T))$ versus T^{-1} . These measurements were performed on MOF films of ~ 130 nm thickness grown on borosilicate glass substrate by an Ecopia HMS-5300 measurement system, Ref.^[28]

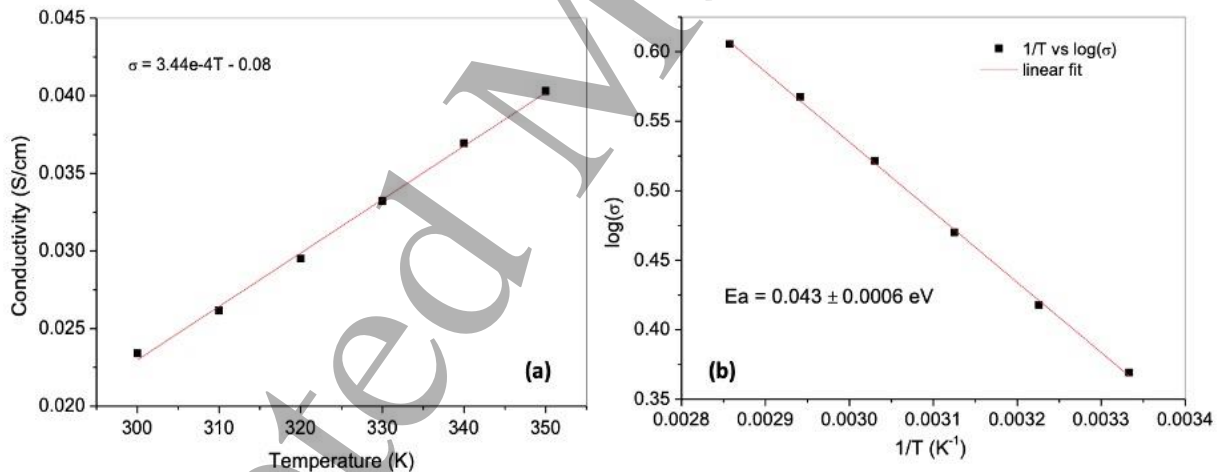


Fig. 11 (a) Plot of the electrical conductivity σ as a function of temperature of TCNQ loaded SURMOF film grown on thick 40 nm isolation SiO_2 covered Si substrates. (b) Arrhenius plot of $\ln(\sigma(T))$ versus T^{-1} , Ref.^[28]